J. Fluid Mech. (1989), *vol.* 203, *pp.* 525–540
Printed in Great Britain

Stationary instability of the convective flow between differentially heated vertical planes

By P. G. DANIELS
Department of Mathematics, The City University, Northampton Square, London EC1V 0HB, UK

(Received 21 March 1988 and in revised form 23 December 1988)

An asymptotic theory describes the stationary instability of convective flow between differentially heated vertical planes at large Prandtl numbers. The theory is concerned with the structure for $A \gg 1$ where A is a Rayleigh number based on the horizontal temperature difference and the distance between the planes. As such it is relevant to the instability of flow in a vertical slot of aspect ratio $h \gg 1$ where the convective regime corresponds to order-one values of a non-dimensional parameter γ which partly depends on the vertical temperature gradient generated in the slot and can be approximated by $\gamma^4 = A/8h$. Instability is shown to set in at a critical value of γ that compares well with experimental observation. The lower branch of the neutral curve conforms to a boundary-layer type approximation while the upper branch has a critical-layer structure midway between the planes which becomes fully developed as the first reversal of the vertical velocity of the base flow is encountered near the centreline.

1. Introduction

Convective flows in two-dimensional vertical slots where one side is held at a different temperature from the other are found in a variety of insulation and heat exchange processes. Experiments by Elder (1965), Vest & Arpaci (1969) and Seki, Fukusako & Inaba (1978) have shown that a prominent feature of such flows is the onset of a secondary motion where transverse rolls are generated within the main circulation driven by the horizontal temperature difference. The basic nature of the flow in the slot depends on three non-dimensional parameters: the aspect ratio h (height/width), a Rayleigh number A based on the horizontal temperature difference and slot width (and defined explicitly in (2.4) below) and the Prandtl number of the fluid, σ. The aspect ratio h is generally assumed to be large. When $A \ll h$ and provided the flow remains stable, heat is transferred across the slot mainly by conduction. Stability analyses of this regime show that the conductive state can be destroyed either by time-dependent or stationary instability depending on whether σ is greater or less than about 12.7 (Korpela, Gozum & Baxi 1973), and in the latter case the instability is actually an imperfect bifurcation of the base flow (Daniels 1985*a*). Both instabilities are avoided, however, if the Prandtl number of the fluid is sufficiently large and the flow enters a single-cell convective regime if $A \gtrsim 645h$. A characteristic feature of this regime is the development of a positive vertical temperature in the fluid. Elder (1965) showed that this could be incorporated in a simple exact solution of the Boussinesq equations which could be used to model the

behaviour of the base flow, albeit in an approximate sense, away from the ends of the slot. The solution depends on the single combination of parameters

$$\gamma = (\tfrac{1}{4}\beta A)^{\frac{1}{4}}, \tag{1.1}$$

where β is a non-dimensional measure of the vertical temperature gradient which can usefully be approximated by the value

$$\beta = \frac{1}{2h} \tag{1.2}$$

(Elder 1965). Elder's experiments, using large-Prandtl-number fluids, demonstrated that the main convective circulation initially becomes unstable to a stationary pattern of vertically stacked transverse rolls.

The main aim of the present work is to determine the point at which instability occurs and the subsequent structure of the neutral curve for stationary disturbances. Previous studies based on Elder's solution, the most comprehensive of which is that by Bergholz (1978), which corrected and extended the earlier analysis of Vest & Arpaci (1969), have regarded γ, as defined by (1.1), and A as independent parameters; the base flow is fixed by the former and the stability problem, which depends also on both A and σ, is solved to yield a critical Rayleigh number A_c. A numerical value of the aspect ratio of the corresponding vertical slot is deduced from (1.1) and (1.2). From an asymptotic viewpoint, however, if the value of h is large and the value of γ is finite, (1.1) and (1.2) imply that the appropriate stability problem is that for which A is large, and it is this alternative interpretation that forms the basis of the present study. The basic state and stability equations are set out in §2. For a fluid of infinite Prandtl number it has already been established that as $A \to \infty$ one branch of neutrally stable solutions corresponds to long-wavelength disturbances described by a boundary-layer-type approximation to the stability equations (Daniels 1987). Some additional results are contained in §3. In §4 the asymptotic structure for disturbance wavelengths that remain finite as $A \to \infty$ is described. A critical value $\gamma = \gamma_c$ at which stationary convection first occurs in a fluid of infinite Prandtl number is confirmed, and for $\gamma > \gamma_c$ the location of an upper branch of the neutral curve is established (§5). The results are discussed briefly in §6.

2. Formulation

Consider a fluid layer bounded by infinite rigid vertical planes $x^* = \pm\frac{1}{2}l^*$ maintained at temperatures

$$T^* = T_0^* + \Delta T^* \left(\beta \frac{z^*}{l^*} \pm \frac{1}{2}\right) \quad (x^* = \pm\tfrac{1}{2}l^*), \tag{2.1}$$

where $T_0^*, \Delta T^*$ and β are constants and z^* is the vertical coordinate. Two-dimensional steady motion between the planes at infinite Prandtl number and in the Boussinesq approximation is governed by the non-dimensional equations

$$\nabla^4 \psi = A \frac{\partial T}{\partial x}, \tag{2.2}$$

$$\nabla^2 T = \frac{\partial(T, \psi)}{\partial(x, z)}. \tag{2.3}$$

Here ψ and T are the stream function and temperature non-dimensionalized by the

thermal diffusivity κ and ΔT^* respectively, while the coordinates x, z are non-dimensionalized by l^*. The Rayleigh number A is defined by

$$A = \beta^* g \Delta T^* l^{*3}/\kappa\nu, \tag{2.4}$$

where β^* is the coefficient of thermal expansion, g is the acceleration due to gravity and ν is the kinematic viscosity of the fluid. The boundary conditions at the vertical planes are

$$\psi = \frac{\partial\psi}{\partial x} = 0, \quad T = \beta z \pm \tfrac{1}{2} \quad (x = \pm\tfrac{1}{2}) \tag{2.5}$$

and the non-dimensional velocity field is given in terms of the stream function by

$$u = \frac{\partial\psi}{\partial z}, \quad w = -\frac{\partial\psi}{\partial x}. \tag{2.6}$$

The exact solution of interest here is the vertical two-way flow defined by

$$\psi = A\Psi(x), \quad T = \beta z + \Theta(x), \tag{2.7}$$

where, from (2.2), (2.3)
$$\Psi^{\mathrm{iv}} = \Theta', \Theta'' + 4\gamma^4\Psi' = 0, \tag{2.8}$$

where γ is defined by (1.1) and, from (2.5)

$$\Psi = \Psi' = 0, \quad \Theta = \pm\tfrac{1}{2} \quad (x = \pm\tfrac{1}{2}). \tag{2.9}$$

The solutions for Ψ and Θ are even and odd functions of x respectively and can be written

$$\Psi = \gamma^{-3}(D + D_+ \cosh\gamma x \cos\gamma x + D_- \sinh\gamma x \sin\gamma x), \tag{2.10}$$

$$\Theta = 2(D_- - D_+)\sinh\gamma x \cos\gamma x - 2(D_+ + D_-)\cosh\gamma x \sin\gamma x, \tag{2.11}$$

where
$$\left.\begin{aligned} D_\pm &= -(\cosh\tfrac{1}{2}\gamma \sin\tfrac{1}{2}\gamma \pm \sinh\tfrac{1}{2}\gamma \cos\tfrac{1}{2}\gamma)/8d, \\ D &= (\sinh\gamma + \sin\gamma)/16d, \end{aligned}\right\} \tag{2.12}$$

and $d = \sinh^2\tfrac{1}{2}\gamma + \sin^2\tfrac{1}{2}\gamma$. The limit $\gamma \to 0$ corresponds to the conductive regime where (Batchelor 1954)

$$\Theta \sim x, \quad \Psi \sim \tfrac{1}{24}(x^2 - \tfrac{1}{4})^2 \tag{2.13}$$

and there is upflow for $x > 0$ and downflow for $x < 0$. As γ increases the first notable development is an inversion of the horizontal temperature gradient, which becomes negative near the centreline $x = 0$ when $\gamma = \gamma_a = 4.73$; further inversions $\Theta'(0) = 0$ are given, from (2.11), by the zeros of $\tanh\tfrac{1}{2}\gamma + \tan\tfrac{1}{2}\gamma$. The first flow reversal near the centreline occurs when $\gamma = \gamma_b = 7.85$ and further reversals, $\Psi''(0) = 0$, are given, from (2.10), by the zeros of $\tanh\tfrac{1}{2}\gamma - \tan\tfrac{1}{2}\gamma$. As $\gamma \to \infty$ the oscillations compress into 'buoyancy layers' near each vertical plane and the intervening core region is left vertically stratified and motionless. Near the cold plane, the buoyancy-layer solution obtained from (2.10)–(2.12) is

$$\Theta \sim -\tfrac{1}{2}e^{-X}\cos X, \quad \Psi' \sim \tfrac{1}{4}\gamma^{-2}e^{-X}\sin X, \tag{2.14}$$

where $X = \gamma(x + \tfrac{1}{2})$. Profiles of the velocity and temperature at various values of γ are displayed by Bergholz (1978). Previous stability analyses of the boundary-layer regime ($\gamma \to \infty$) include those by Gill & Davey (1969) and Daniels (1985*b*) and, for unit Prandtl number, instabilities of rotating Poiseuille flow discussed by Wollkind & DiPrima (1973) and in the Ekman-layer limit by Lilly (1966) would also be relevant.

The present paper is concerned with the structure of neutrally stable, stationary

disturbances to the above state which can be represented in normal-mode form by solutions

$$\psi \sim A(\Psi(x)+\phi(x)\,\mathrm{e}^{\mathrm{i}\alpha z}), \quad T \sim \beta z+\Theta(x)+\theta(x)\,\mathrm{e}^{\mathrm{i}\alpha z}, \tag{2.15}$$

where α is the vertical wavenumber. Substitution into (2.2), (2.3) and linearization in the perturbation functions ϕ and θ yields the coupled system

$$\phi^{\mathrm{iv}}-2\alpha^2\phi''+\alpha^4\phi = \theta', \tag{2.16}$$

$$\theta''-\alpha^2\theta = \mathrm{i}\alpha A(\Theta'\phi-\Psi'\theta)-4\gamma^4\phi', \tag{2.17}$$

to be solved subject to $$\phi = \phi' = \theta = 0 \quad (x = \pm\tfrac{1}{2}). \tag{2.18}$$

Solutions for finite values of γ and A are included in the results obtained by Bergholz (1978); here the aim is to identify the asymptotic structure for large A which, as explained earlier, is of primary significance in applications to vertical-slot flows. Before proceeding with this in §3 it is worth noting some relevant general properties of (2.16)–(2.18). First, if α is an eigenvalue associated with eigenfunctions $\phi(x), \theta(x)$ then $-\alpha$ is also an eigenvalue, associated with $\phi(-x), -\theta(-x)$. Second, if α is complex then $-\alpha^*$ is also an eigenvalue, associated with eigenfunctions $\phi^*(x), \theta^*(x)$, so that consideration of (2.16)–(2.18) may be restricted to the first quadrant of the complex-α plane. The main interest is in neutrally stable solutions where α is real but spatially decaying solutions with $\mathrm{Im}\,(\alpha) \neq 0$ are also relevant to the flow near the ends of a vertical slot in the conductive regime ($\gamma = 0$) and previous results (Daniels 1985*a*) provide a useful guide to the behaviour of the eigenvalues at higher values of γ. Where real values of α do occur, the symmetry properties of (2.16)–(2.18) allow the eigenfunctions to be expressed in the form

$$\phi = \phi^{(\mathrm{o})}+\mathrm{i}\phi^{(\mathrm{e})}, \quad \theta = \theta^{(\mathrm{e})}+\mathrm{i}\theta^{(\mathrm{o})}, \tag{2.19}$$

where $\phi^{(\mathrm{o})}, \theta^{(\mathrm{o})}$ and $\phi^{(\mathrm{e})}, \theta^{(\mathrm{e})}$ are real odd and even functions of x respectively.

3. The lower branch of the neutral curve

One set of solutions of (2.16)–(2.18) arises for long wavelengths such that

$$\alpha \sim \bar{\alpha}A^{-1} \quad \text{as } A \to \infty, \tag{3.1}$$

where $\bar{\alpha}$ is finite. In this case the leading approximations to the stability equations and boundary conditions are

$$\bar{\phi}^{\mathrm{iv}} = \bar{\theta}', \tag{3.2}$$

$$\bar{\theta}''+4\gamma^4\bar{\phi}' = \mathrm{i}\bar{\alpha}(\Theta'\bar{\phi}-\Psi'\bar{\theta}), \tag{3.3}$$

$$\bar{\phi} = \bar{\phi}' = \bar{\theta} = 0 \quad (x = \pm\tfrac{1}{2}), \tag{3.4}$$

where $\phi \sim \bar{\phi}(x)$ and $\theta \sim \bar{\theta}(x)$ as $A \to \infty$. In an earlier study (Daniels 1987) it was established that real eigenvalues $\bar{\alpha}$ exist for $\gamma > \gamma_{\mathrm{c}}$ where γ_{c} is the lowest value of γ for which the system

$$f'''-\frac{\Theta'}{\Psi'}f = 0; \quad f = f' = 0, \quad f'' = 1 \quad (x = -\tfrac{1}{2}) \tag{3.5}$$

has a solution in $-\frac{1}{2} \leqslant x \leqslant 0$ with

$$b = f'(0) = 0. \tag{3.6}$$

The value of γ_{c} must be greater than $\gamma_{\mathrm{a}} = 4.73$ since otherwise $\Theta'/\Psi' > 0$ and f' is an increasing function of x. The most accurate numerical results gave a first zero of b at

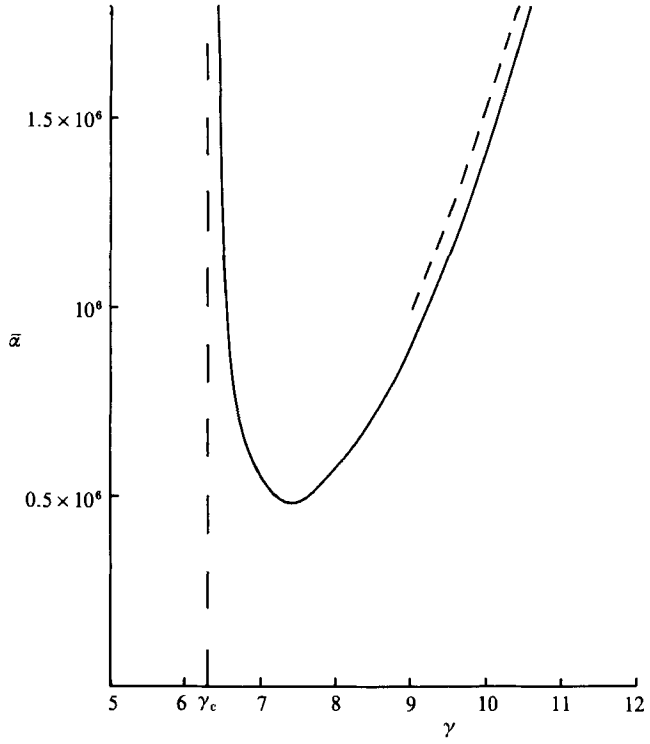

FIGURE 1. The lower branch of the neutral curve and the asymptote (3.10).

$\gamma_c = 6.30$ and while it is tempting to conjecture that the value is exactly 2π, which would correspond to the first maximum (for variations in γ) of the centreline stream-function value

$$\psi = A^{\frac{1}{4}}(4\beta)^{-\frac{3}{4}}\left(\frac{\sinh\frac{1}{2}\gamma - \sin\frac{1}{2}\gamma}{\cosh\frac{1}{2}\gamma + \cos\frac{1}{2}\gamma}\right) \tag{3.7}$$

of the base flow, this result has not been established. Further investigation has indicated that additional zeros of b occur near $\gamma_b = 7.85$. The nature of the singularity of (3.5) at $x = 0$ changes when $\gamma = \gamma_b$ since at this point the general behaviour $\Theta'/\Psi' = O(x^{-1})$ as $|x| \to 0$ is replaced by $\Theta'/\Psi' \sim 6x^{-3}$ leading to the oscillatory form

$$f \sim c_1 \sin(\sqrt{2}\ln|x| + c_2) \quad \text{as } x \to 0-. \tag{3.8}$$

The exponential character of the local coordinate is consistent with the occurrence of zeros of (3.6) very close to γ_b and later results (§4) confirm the existence of an intricate structure in the immediate vicinity of this point.

Figure 1 shows the real eigenvalue $\bar{\alpha}$ plotted as a function of γ which, as is demonstrated below, can be interpreted as the lower branch of a neutral stability curve. As $\gamma \to \gamma_c+$ the value of $\bar{\alpha}$ increases and a critical layer of thickness $\bar{\alpha}^{-\frac{1}{3}}$ forms on the centreline $x = 0$. An asymptotic analysis indicates that

$$\bar{\alpha} \sim \bar{\alpha}_0(\gamma - \gamma_c)^{-1} \quad (\bar{\alpha}_0 \text{ constant}), \tag{3.9}$$

and at leading order provides the value of γ_c from the outer equation (3.5) and the condition (3.6), which results from the relevant bridging conditions across the critical layer. Consideration of correction terms to the analysis given by Daniels (1987)

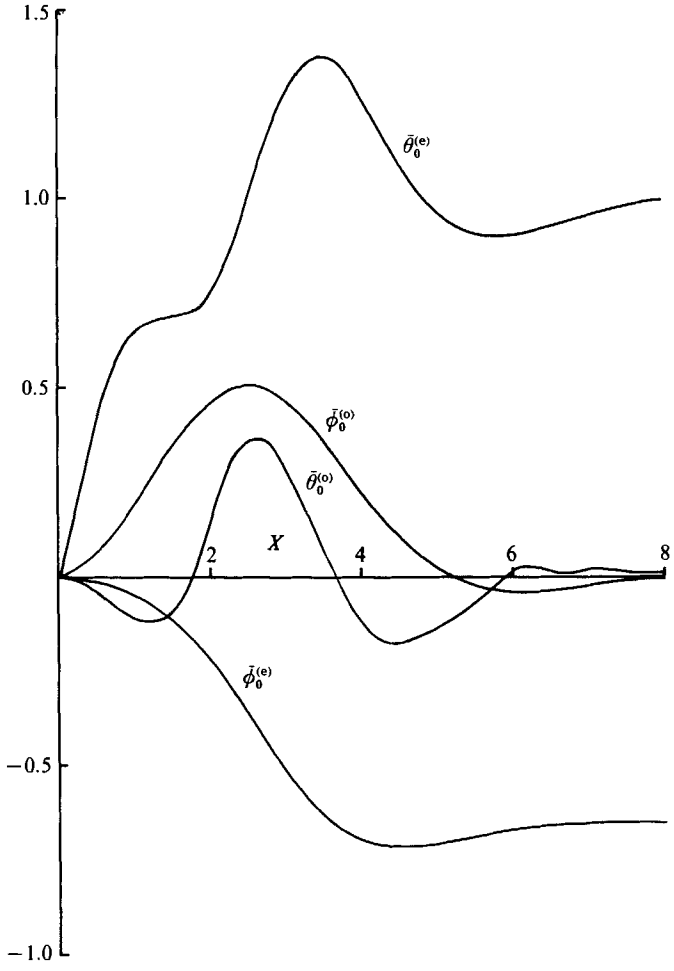

FIGURE 2. Buoyancy-layer profiles of stream function and temperature.

suggests the inverse power-law dependence (3.9), due essentially to the reaction produced by the terms on the left-hand side of (3.3) outside the critical layer. These are neglected at leading order but produce an effect of relative order $\bar{\alpha}^{-1}$ which must be balanced by a correction to the value of γ of the same order of magnitude. The actual determination of $\bar{\alpha}_0$ is extremely lengthy, however, and is reserved for future consideration.

At larger values of γ,

$$\bar{\alpha} \sim \bar{\alpha}_1 \gamma^4 \quad (\bar{\alpha}_1 \text{ constant}), \tag{3.10}$$

where $\bar{\alpha}_1 \approx 152.3$ (Daniels 1987). Here the full balance in (3.2), (3.3) is achieved in the buoyancy layers where $x \pm \frac{1}{2} = O(\gamma^{-1})$ and

$$\bar{\theta} \sim \bar{\theta}_0^{(e)} + \mathrm{i}\bar{\theta}_0^{(o)}, \quad \bar{\phi} \sim \gamma^{-3}(\bar{\phi}_0^{(o)} + \mathrm{i}\bar{\phi}_0^{(e)}). \tag{3.11}$$

The solutions approach constant limiting values in the core given by

$$\bar{\theta} \sim 1, \quad \bar{\phi} \sim \mathrm{i}\lambda\gamma^{-3}, \tag{3.12}$$

where the symmetry forms (2.19) imply that λ must be real. Numerical solution of the buoyancy-layer problem at the cold wall (Daniels 1985*b*) gives $\lambda = -0.65$ and the

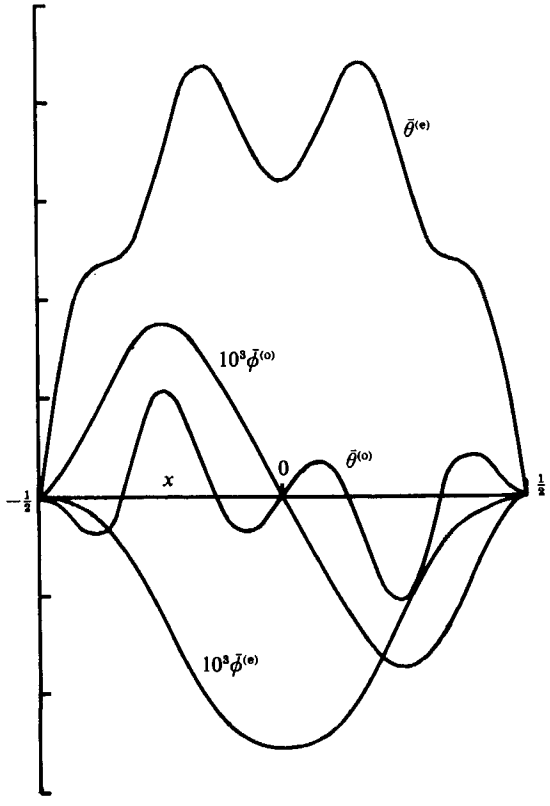

FIGURE 3. Stream function and temperature profiles for the lower branch of the neutral curve at $\gamma = 10$, expressed in the symmetry forms $\bar{\phi} = \bar{\phi}^{(o)} + i\bar{\phi}^{(e)}, \bar{\theta} = \bar{\theta}^{(e)} + i\bar{\theta}^{(o)}$.

above value of $\bar{\alpha}_1$. The neutral disturbance consists of large rolls in which the circulation through the buoyancy layers is linked by horizontal flow across the core; the boundary-layer profiles (3.11) are shown in figure 2.

Typical stream function and temperature profiles for the lower branch of the neutral curve, at $\gamma = 10$, are shown in figure 3; note the central variation of $\bar{\phi}^{(o)}$ absent in the boundary-layer limit, which indicates that at lower values of γ the roll boundaries slant up towards the hotter plane, consistent with experimental observations.

It should be added that the reduced system (3.2)–(3.4) also admits an infinite set of imaginary eigenvalues. These are related to the vertical spatial variation of the base flow of the convective regime in a vertical slot (Daniels 1987).

4. The structure for $A \gg 1$: finite wavelengths

Solutions for which α remains finite as $A \to \infty$ require basic expansions in powers of $A^{-\frac{1}{3}}$, the thickness of a critical layer on the slot centreline. Thus

$$\alpha \sim \alpha_0 + A^{-\frac{1}{3}}\alpha_1 \quad \text{as } A \to \infty, \tag{4.1}$$

and an outer solution is needed in the form

$$\left.\begin{aligned} \phi &\sim \phi_0(x) + A^{-\frac{1}{3}}\phi_1(x), \\ \theta &\sim \theta_0(x) + A^{-\frac{1}{3}}\theta_1(x). \end{aligned}\right\} \tag{4.2}$$

From (2.17),
$$\theta_0 = \frac{\Theta'}{\Psi'}\phi_0, \tag{4.3}$$

and substitution into (2.16) gives the fourth-order equation

$$\phi_0^{\mathrm{iv}} - 2\alpha_0^2\phi_0'' + \alpha_0^4\phi_0 = \frac{\mathrm{d}}{\mathrm{d}x}\left(\frac{\Theta'}{\Psi'}\phi_0\right), \tag{4.4}$$

for ϕ_0. At the vertical planes the conditions

$$\phi_0 = \phi_0' = 0 \quad (x = \pm\tfrac{1}{2}), \tag{4.5}$$

together with (4.3), ensure that both the flow and thermal boundary conditions are satisfied to leading order, although boundary layers of thickness order $A^{-\frac{1}{3}}$ provide adjustments to higher-order terms.

At the centreline $x = 0$, the solution of (4.4) generally contains a logarithmic singularity due to the vanishing of the base-flow velocity Ψ', so that

$$\phi_0 \sim a^{\pm} + b^{\pm}x + x^2\left(\frac{\mu}{2\omega}a^{\pm}\ln|x| + c^{\pm}\right) + d^{\pm}x^3 + O(x^4\ln|x|) \quad \text{as } x \to 0\pm, \tag{4.6}$$

where $a^{\pm}, \ldots d^{\pm}$ are independent complex constants. The real constants μ and ω arise from the behaviour of the base state as $|x| \to 0$,

$$\Theta' = -\mu + O(x^2), \quad \Psi' = -\omega x + O(x^3) \tag{4.7}$$

and, from (2.10), (2.11), are given by

$$\mu = -\tfrac{1}{2}\gamma\left(\frac{\sinh\frac{1}{2}\gamma\cos\frac{1}{2}\gamma + \cosh\frac{1}{2}\gamma\sin\frac{1}{2}\gamma}{\sinh^2\frac{1}{2}\gamma + \sin^2\frac{1}{2}\gamma}\right), \quad \omega = \frac{1}{4\gamma}\left(\frac{\cosh\frac{1}{2}\gamma\sin\frac{1}{2}\gamma - \sinh\frac{1}{2}\gamma\cos\frac{1}{2}\gamma}{\sinh^2\frac{1}{2}\gamma + \sin^2\frac{1}{2}\gamma}\right). \tag{4.8}$$

The value of ω is positive for $\gamma < \gamma_b$ while μ changes sign from negative to positive at γ_a. If $a^{\pm}$ are non-zero a critical layer of thickness order $A^{-\frac{1}{3}}$ is needed to smooth out the singularity in (4.6) and local expansions for the stream function and temperature there are

$$\left.\begin{aligned} \phi &= \tilde{\phi}_0(\xi) + A^{-\frac{1}{3}}\tilde{\phi}_1(\xi) + A^{-\frac{2}{3}}\ln A\tilde{\phi}_{20}(\xi) + A^{-\frac{2}{3}}\tilde{\phi}_2(\xi) + A^{-1}\tilde{\phi}_3(\xi) + \ldots, \\ \theta &= A^{\frac{1}{3}}\tilde{\theta}_0(\xi) + \tilde{\theta}_1(\xi) + \ldots, \end{aligned}\right\} \tag{4.9}$$

where $\xi = A^{\frac{1}{3}}x$. Substitution into (2.16) and matching with (4.6) leads successively to the results

$$\left.\begin{aligned} &\tilde{\phi}_0 = a^+ = a^-, \quad \tilde{\phi}_1' = b^+ = b^-, \quad \tilde{\phi}_{20}'' = -\frac{\mu}{3\omega}a^+, \\ &\tilde{\phi}_3''' \doteq \tilde{\theta}_1 + \text{constant}, \end{aligned}\right\} \tag{4.10}$$

together with
$$\lim_{\Delta\to\infty}(\tilde{\phi}_2''(\Delta) - \tilde{\phi}_2''(-\Delta)) = \int_{-\infty}^{\infty}\tilde{\theta}_0(\xi')\,\mathrm{d}\xi', \tag{4.11}$$

where $\tilde{\theta}_0 = a^+\mu\omega^{-\frac{2}{3}}\tilde{\theta}(\tilde{\xi})$, $\tilde{\xi} = \omega^{\frac{1}{3}}\xi$ and $\tilde{\theta}$ is the solution of

$$\tilde{\theta}'' - \mathrm{i}\alpha_0\tilde{\xi}\tilde{\theta} = -\mathrm{i}\alpha_0; \quad \tilde{\theta} \sim \tilde{\xi}^{-1} \quad (|\tilde{\xi}| \to \infty) \quad (\mathrm{Re}\,(\alpha_0) \neq 0). \tag{4.12}$$

A Fourier transformation gives

$$\tilde{\theta} = \mathrm{i}\int_0^{\infty}\exp\left(-\frac{p^3}{3\alpha_0} - \mathrm{i}p\tilde{\xi}\right)\mathrm{d}p \quad (\mathrm{Re}\,(\alpha_0) > 0), \tag{4.13}$$

from which the integral in (4.11) is evaluated as $i\pi a^+\mu/\omega$ and it now follows that the bridging conditions across the critical layer are

$$a^+ = a^-, \quad b^+ = b^-, \quad c^+ = c^- + \frac{i\pi\mu a^+}{2\omega}, \quad d^+ = d^-. \tag{4.14}$$

The fourth one uses the fact that $\tilde{\theta}_1$ in (4.10) must match with θ_0 in the outer expansion, the finite part of which is continuous across the layer, from (4.3).

Solutions of the outer problem (4.4), (4.5) in $x < 0$ are constructed in the form

$$\phi_0 = \nu_1^- f_1(x) + \nu_2^- f_2(x), \tag{4.15}$$

where $\nu_{1,2}^-$ are complex constants and the functions f_1 and f_2 satisfy

$$f_{1,2}^{iv} - 2\alpha_0^2 f_{1,2}'' + \alpha_0^4 f_{1,2} = \frac{d}{dx}\left(\frac{\Theta'}{\Psi'} f_{1,2}\right) \tag{4.16}$$

and are uniquely defined for $-\frac{1}{2} \leqslant x \leqslant 0$ by the conditions

$$\left.\begin{aligned} f_1 = f_1' = f_1''' = 0, \quad f_1'' = 1 \\ f_2 = f_2' = f_2'' = 0, \quad f_2''' = 1 \end{aligned}\right\} \quad \text{at } x = -\tfrac{1}{2}. \tag{4.17}$$

As $x \to 0-$, $$f_i \sim a_i + b_i x + x^2\left\{\frac{a_i\mu}{2\omega}\ln|x| + c_i\right\} + d_i x^3 \quad (i = 1, 2) \tag{4.18}$$

and since the symmetry of the base functions implies that the solution for ϕ_0 in $x > 0$ can be written

$$\phi_0 = \nu_1^+ f_1(-x) + \nu_2^+ f_2(-x), \tag{4.19}$$

where $\nu_{1,2}^+$ are further complex constants, the bridging conditions (4.14) become

$$(\nu_1^- - \nu_1^+)\, a_1 + (\nu_2^- - \nu_2^+)\, a_2 = 0, \tag{4.20a}$$

$$(\nu_1^- + \nu_1^+)\, b_1 + (\nu_2^- + \nu_2^+)\, b_2 = 0, \tag{4.20b}$$

$$(\nu_1^- - \nu_1^+)\, c_1 + (\nu_2^- - \nu_2^+)\, c_2 = -i\pi\mu(\nu_1^+ a_1 + \nu_2^+ a_2)/2\omega, \tag{4.20c}$$

$$(\nu_1^- + \nu_1^+)\, d_1 + (\nu_2^- + \nu_2^+)\, d_2 = 0. \tag{4.20d}$$

Two sets of solutions are obtained. In the first ϕ_0 is non-zero on the centreline and (4.20*b*, *d*) give

$$b_1 d_2 - b_2 d_1 = 0. \tag{4.21}$$

In the second the solution for ϕ_0 is odd and the singularity is avoided; in this case $\nu_{1,2}^+ = -\nu_{1,2}^-$ and (4.20*a*, *c*) give

$$a_1 c_2 - c_1 a_2 = 0. \tag{4.22}$$

For a given value of γ, the real and imaginary parts of α_0 must be chosen to ensure that the real and imaginary parts of either (4.21) or (4.22) are satisfied.

Solutions were found numerically by using a fourth-order Runge–Kutta scheme to solve (4.16), (4.17) at given values of α_0 and γ; the initial step at $x = -\frac{1}{2}$ was accomplished by use of a Taylor series and solutions for f_1 and f_2 were computed, generally with either 40 or 80 steps, to within one step of the singularity at $x = 0$. An accurate determination of the constants a_i, b_i, c_i, d_i proved to be vital in locating the correct paths of the eigenvalues in the complex-α_0 plane and an extrapolation based on (4.18) could not determine the value of d_i sufficiently accurately. Instead, it was found necessary to introduce the two integral forms

$$I_i = \int_{-\frac{1}{2}}^{0} f_i \, dx \quad (i = 1, 2) \tag{4.23}$$

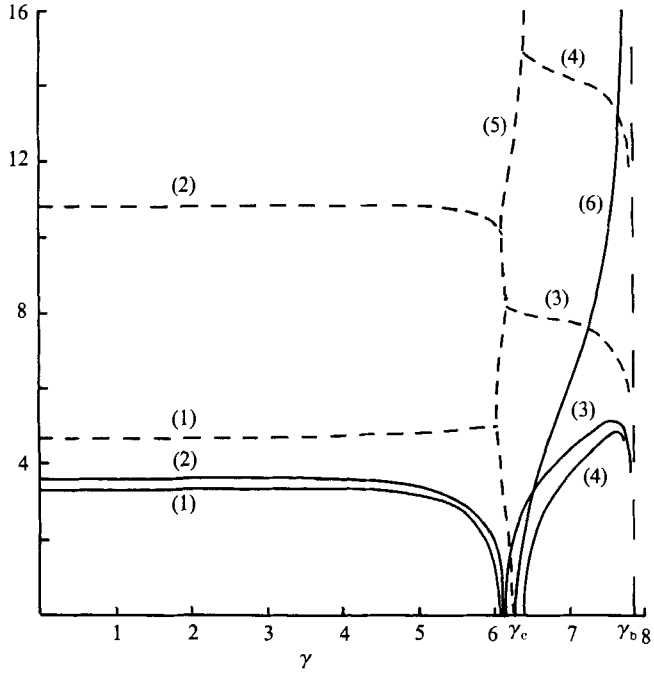

FIGURE 4. Eigenvalues α_0 obtained from (4.24): real part (——), imaginary part (– – –). Different branches are labelled (1)...(6). Section (5) is purely imaginary. Section (6) from $\gamma_c = 6.30$ to $\gamma_b = 7.85$ is purely real and constitutes the upper branch of the neutral curve.

and it is then easily shown by integration of (4.16) and use of (4.17) that the condition (4.21) becomes

$$b_1 + \alpha_0^4(b_2 I_1 - b_1 I_2) = 0. \tag{4.24}$$

Direct computation of $d_{1,2}$ is avoided and accurate numerical values of the integrals (4.23) are easily obtained.

The zeros of (4.24) or (4.22) were found for a fixed value of γ by Newton iteration based on a numerical determination of the rates of change of their real and imaginary parts. Convergence of the value of α_0 could generally be achieved within four or five iterations, given reasonable initial estimates of its real and imaginary parts. Solutions were initiated at the conductive state, for which $\gamma = 0$. Here solutions of (2.16)–(2.18) for general values of A are related to the decay properties of the flow near the ends of a vertical slot and have been reported in that context by the present author (1985*a*). As $A \to \infty$, one set of eigenvalues adopts the scaling $\alpha = O(A^{-1})$, consistent with the results of §3, while the other sets remain finite and must tend to values consistent with the results of the present computation at $\gamma = 0$; both the leading eigenvalue obtained from (4.24) ($\alpha_0 = 3.26 + 4.67\mathrm{i}$) and the first odd eigenvalue obtained from (4.22) ($\alpha_0 = 2.30 + 7.43\mathrm{i}$) are, indeed, in excellent agreement with these earlier results. Figures 4 and 5 show the development of the first four eigenvalues as γ increases to the point at which the base flow reverses on the centreline ($\gamma_b = 7.85$). At $\gamma \approx 6.1$ the real part of the leading eigenvalue falls to zero and a purely imaginary branch joins successive modes emanating from the conductive state at $\gamma = 0$. This in turn reaches zero at $\gamma = \gamma_c = 6.30$ whereupon the real part is regenerated to form the upper branch of the neutral curve stemming from γ_c. Its properties are discussed in the next section but it is now clear that as $A \to \infty$,

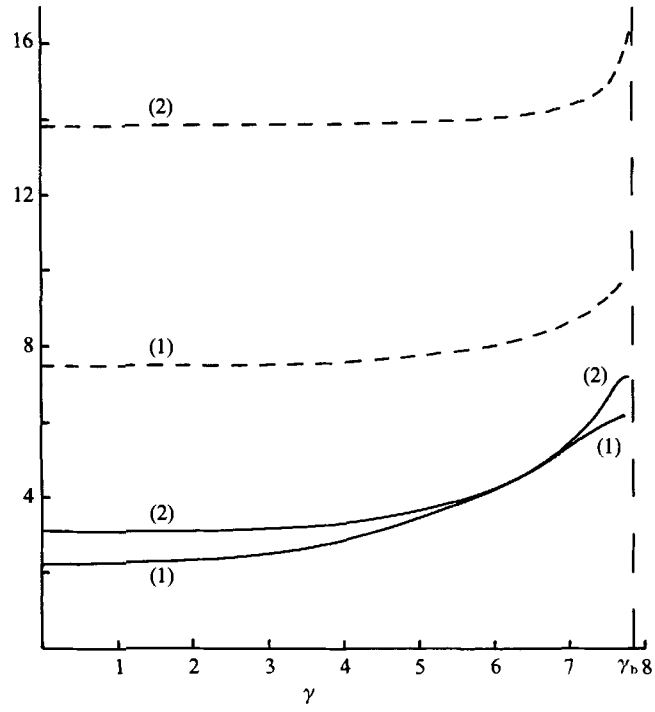

FIGURE 5. Eigenvalues α_0 obtained from (4.22): real part (——), imaginary part (– – – –). Different branches are labelled (1), (2).

γ_c is the critical point of stationary instability of the infinite-Prandtl-number flow for the entire range of vertical wavelengths (see figure 8 below).

5. The upper branch of the neutral curve

Near γ_c the properties of the base flow are defined by regular expansions

$$(\Theta, \Psi, \mu, \omega) \sim (\Theta_0, \Psi_0, \mu_0, \omega_0) + (\gamma - \gamma_c)(\Theta_1, \Psi_1, \mu_1, \omega_1), \tag{5.1}$$

and the behaviour of the leading eigenvalue of figure 4 may be investigated by assuming that

$$\alpha_0^2 \sim a(\gamma - \gamma_c) \quad \text{as } \gamma \to \gamma_c, \tag{5.2}$$

where a is an unknown complex constant. The existence of the critical point of the reduced system (3.5), (3.6) ensures that such a point exists where both the real and imaginary parts of the eigenvalue α_0 vanish simultaneously; the zero of α_0^2 is linear because the governing equations (4.16) depend only on the square of α_0. Near γ_c,

$$(f_{1,2}, b_{1,2}) = (f_{10,20}, b_{10,20}) + (\gamma - \gamma_c)(f_{11,21}, b_{11,21}) + \ldots. \tag{5.3}$$

The condition (4.24) implies $$b_{10} = f'_{10}(0) = 0, \tag{5.4}$$

where, from (4.16), f_{10} is the solution of

$$f'''_{10} - \frac{\Theta'_0}{\Psi'_0} f_{10} = 0; \quad f_{10} = f'_{10} = 0, \quad f''_{10} = 1 \quad (x = -\tfrac{1}{2}). \tag{5.5}$$

Thus $f_{10} = f|_{\gamma_c}$, consistent with the determination of γ_c from the equivalent reduced system (3.5), (3.6).

Consideration of the correction terms in (5.1)–(5.3) enables some predictions to be made concerning the departure of the neutral curve from the neighbourhood of γ_c. Again the crucial information is obtained ultimately from the first of the equations (4.16) which requires that f_{11} satisfies

$$f_{11}''' - \frac{\Theta_0'}{\Psi_0'} f_{11} = \left(\frac{\Theta_1' \Psi_0' - \Psi_1' \Theta_0'}{\Psi_0'^2} \right) f_{10} + 2a f_{10}', \tag{5.6}$$

where

$$f_{11} = f_{11}' = f_{11}'' = 0 \quad (x = -\tfrac{1}{2}). \tag{5.7}$$

Also, from (4.24),

$$b_{11} = f_{11}'(0) = 0. \tag{5.8}$$

Since $f_{11} = \partial f / \partial \gamma |_{\gamma_c}$ is a particular solution of (5.6), (5.7) for $a = 0$ (where f is the solution of (3.5)) and $\mathrm{d}b/\mathrm{d}\gamma |_{\gamma_c} \neq 0$, another particular solution must be generated by a in order to achieve the condition (5.8). The value of a so determined must be real (since f_{10} is real) and the fact that $\mathrm{d}b/\mathrm{d}\gamma |_{\gamma_c} < 0$ indicates that it must be positive. From (5.2), this result confirms the behaviour found in figure 4, where α_0 is imaginary for $\gamma = \gamma_c -$ and real for $\gamma = \gamma_c +$.

At general values of $\gamma \geqslant \gamma_c$ stream function and temperature profiles on the upper branch of the neutral curve are obtained from (4.15) and (4.19) once the complex constants ν_1^+, ν_2^+ and ν_2^- are determined in terms of ν_1^- from (4.20*a–d*). Since α_0 is real the solutions can be converted into the standard form (2.19) by a suitable choice of the arbitrary complex constant ν_1^- and this gives $\phi_0 = \phi_0^{(o)} + \mathrm{i}\phi_0^{(e)}$ where

$$\left.\begin{aligned} \phi_0^{(o)} &= \frac{\mu\pi}{2\omega} (a_2 b_1 - b_2 a_1)(a_1 f_2(x) - a_2 f_1(x)) \\ \phi_0^{(e)} &= 2(a_2 c_1 - c_2 a_1)(b_2 f_1(x) - b_1 f_2(x)), \end{aligned}\right\} \quad \text{for } x < 0. \tag{5.9}$$

The profiles at γ_c, along with the corresponding forms for θ, are shown in figure 6. Note the infinite singularity in θ_0 as $x \to 0\pm$ which is smoothed out by the critical-layer structure, and the fact that at small amplitudes the signs of $\phi_0^{(o)}$ and $\phi_0^{(e)}$ are such that the critical flow will have the form of rolls rotating with the main circulation and skewed upwards to the hotter side, consistent with the observations of Elder (1965), Seki *et al.* (1978) and others.

As the value of γ increases to γ_b the neutral disturbance becomes confined to the neighbourhood of the critical layer and the wavenumber increases. It is found that

$$\alpha_0 \sim c(\gamma_b - \gamma)^{-\frac{1}{2}} \quad \text{as } \gamma \to \gamma_b -, \tag{5.10}$$

where c is a finite constant, and that variations in the outer region are characterized by a local coordinate $\bar{x}$ where

$$x = (\gamma_b - \gamma)^{\frac{1}{2}} \bar{x}. \tag{5.11}$$

The base-flow velocity has the form

$$-\Psi' \sim (\gamma_b - \gamma)^{\frac{3}{2}} (\tfrac{1}{6} \bar{\mu} \bar{x}^3 + \bar{\omega} \bar{x}) \quad \text{as } \gamma \to \gamma_b -, \tag{5.12}$$

where $\bar{\mu} = \mu |_{\gamma_b}$ and $\bar{\omega} = -\mathrm{d}\omega/\mathrm{d}\gamma |_{\gamma_b} > 0$, while the horizontal temperature gradient is given by

$$\Theta' = -\bar{\mu} + O(\gamma_b - \gamma)\, \bar{x}^2) \quad \text{as } \gamma \to \gamma_b -. \tag{5.13}$$

Hence

$$\frac{\Theta'}{\Psi'} \sim 6(\gamma_b - \gamma)^{-\frac{3}{2}} (\bar{x}^3 + \Omega \bar{x})^{-1} \quad \text{as } \gamma \to \gamma_b -, \tag{5.14}$$

where

$$\Omega = \frac{6\bar{\omega}}{\bar{\mu}} = \frac{3}{2\gamma_b^2} \tan(\tfrac{1}{2}\gamma_b) = 0.0243. \tag{5.15}$$

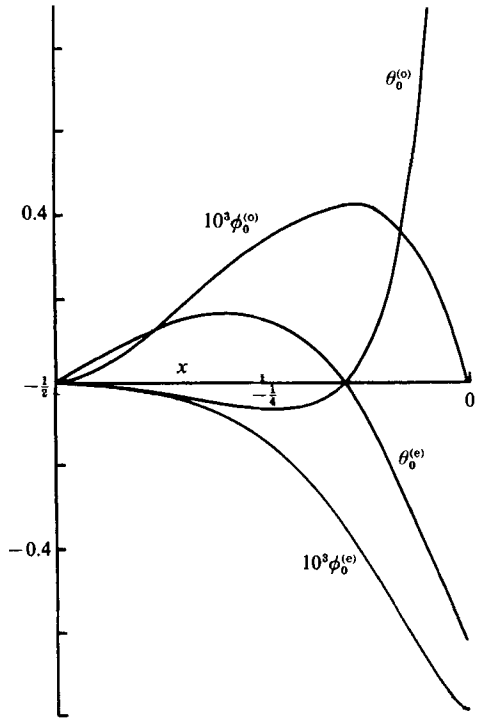

FIGURE 6. Stream function and temperature profiles at the critical point γ_c expressed in the symmetry forms $\phi_0 = \phi_0^{(o)} + i\phi_0^{(e)}, \theta_0 = \theta_0^{(e)} + i\theta_0^{(o)}$.

It is convenient to introduce the transformations

$$c = \Omega^{-\frac{1}{3}}\tilde{c}, \quad \bar{x} = \Omega^{\frac{1}{3}}\tilde{x}, \tag{5.16}$$

whereupon the scaling (5.10), together with (5.11) and the assumption that $\phi_0(x) \sim \tilde{\phi}(\tilde{x})$, ensures that a full balance is retained in the stability equation (4.4), which becomes

$$\tilde{\phi}^{iv} - 2\tilde{c}^2\tilde{\phi}'' + \tilde{c}^4\tilde{\phi} = \frac{d}{d\tilde{x}}\left(\frac{6\tilde{\phi}}{\tilde{x}^3 + \tilde{x}}\right). \tag{5.17}$$

As $\tilde{x} \to -\infty$ independent solutions $\tilde{\phi} = \tilde{f}_1$ and $\tilde{\phi} = \tilde{f}_2$ approach the two available exponentially decaying forms

$$\tilde{f}_1 \sim e^{\tilde{c}\tilde{x}}, \quad \tilde{f}_2 \sim \tilde{x}e^{\tilde{c}\tilde{x}} \quad (\mathrm{Re}\,(\tilde{c}) > 0), \tag{5.18}$$

while as $\tilde{x} \to 0-$

$$\tilde{f}_{1,2} \sim \tilde{a}_{1,2} + \tilde{b}_{1,2}\tilde{x} + \tilde{x}^2(3\tilde{a}_{1,2}\ln|\tilde{x}| + \tilde{c}_{1,2}) + \tilde{d}_{1,2}\tilde{x}^3, \tag{5.19}$$

and the critical-layer bridging condition (4.24) becomes

$$\tilde{b}_2\tilde{I}_1 - \tilde{b}_1\tilde{I}_2 = 0 \quad \text{where } \tilde{I}_{1,2} = \int_{-\infty}^{0} \tilde{f}_{1,2}\,d\tilde{x}. \tag{5.20}$$

A numerical solution located a real eigenvalue of this system at $\tilde{c} = 0.988$, equivalent to an upper-branch asymptote

$$\alpha_0 \sim 6.27\,(\gamma_b - \gamma)^{-\frac{1}{2}} \quad \text{as } \gamma \to \gamma_b -, \tag{5.21}$$

which is in good agreement with the results of figure 4.

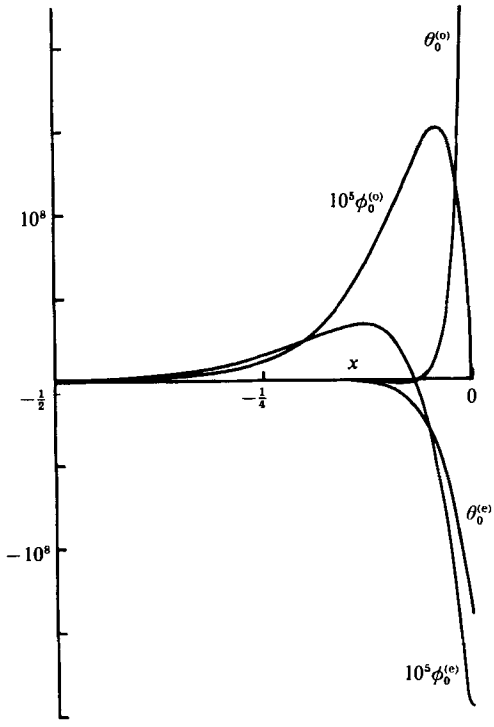

FIGURE 7. Stream function and temperature profiles for the upper branch of the neutral curve at $\gamma = 7.7$, expressed in the symmetry forms $\phi_0 = \phi_0^{(o)} + i\phi_0^{(e)}, \theta_0 = \theta_0^{(e)} = i\theta_0^{(o)}$.

Profiles of ϕ_0 and θ_0 obtained from (5.9) at $\gamma = 7.7$ and shown in figure 7 confirm the confinement of the solution to the neighbourhood of the critical layer. From (4.12), the width of the critical layer is

$$x \sim A^{-\frac{1}{3}}\alpha_0^{-\frac{1}{3}}\omega^{-\frac{1}{3}} \sim A^{-\frac{1}{3}}(\gamma_b - \gamma)^{-\frac{1}{6}}, \tag{5.22}$$

whereas that of the outer zone $\tilde{x} \sim 1$ is equivalent to $x \sim (\gamma_b - \gamma)^{\frac{1}{2}}$. Thus the critical layer contains the entire disturbance when $\hat{\gamma}$, defined by

$$\gamma = \gamma_b + \frac{\bar{\mu}}{\bar{\omega}}(\bar{\mu}A)^{-\frac{1}{2}}\hat{\gamma}, \tag{5.23}$$

is order one and further scalings

$$\alpha \sim (\bar{\mu}A)^{\frac{1}{4}}\hat{\alpha}, \quad x \sim (\bar{\mu}A)^{-\frac{1}{4}}\hat{x}, \quad \phi \sim (\bar{\mu}A)^{-\frac{3}{4}}\hat{\phi}(\hat{x}), \quad \theta \sim \hat{\theta}(\hat{x}), \tag{5.24}$$

lead to the problem of solving the full critical-layer system

$$\left.\begin{aligned} \hat{\phi}^{iv} - 2\hat{\alpha}^2\hat{\phi}'' + \hat{\alpha}^4\hat{\phi} &= \hat{\theta}', \\ \hat{\theta}'' - \hat{\alpha}^2\hat{\theta} &= -i\hat{\alpha}\{\hat{\phi} + (\hat{\gamma}\hat{x} - \tfrac{1}{6}\hat{x}^3)\hat{\theta}\}, \end{aligned}\right\} \tag{5.25}$$

in order to trace the eigenvalue $\hat{\alpha}$ as a function of $\hat{\gamma}$. Note that here the scalings (5.24) imply that the disturbance consists of small vortices of horizontal and vertical dimension order-$A^{-\frac{1}{4}}$ confined to the region of weakest flow at the centreline $x = 0$.

σ	h	$A_c \times 10^{-5}$	$(A_c/h)^{\frac{1}{4}}$	Author
10^3	19	3.0	11.2	Elder (1965)
900	20	3.7	11.7	Vest & Arpaci (1969)
480	15	1.8	10.4	Seki *et al.* (1978)
10	4	0.42	10.1	Simpkins & Dudderar (1981)

TABLE 1. Experimental results for the onset of stationary instability of high-Prandtl-number flow in a vertical slot

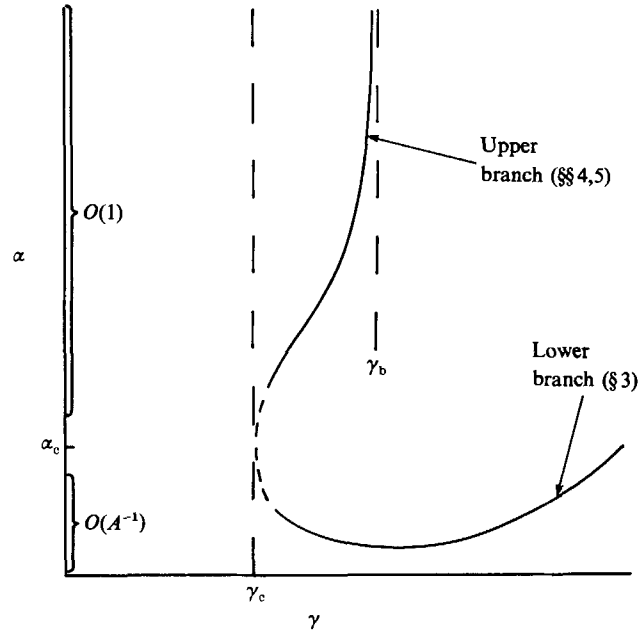

FIGURE 8. Schematic diagram of the structure of the neutral curve in the (γ, α)-plane as $A \to \infty$.

6. Discussion

The present study provides a new interpretation of the stability of high-Prandtl-number flow in vertical slots. The usual procedure in numerical studies based on Elder's (1965) approximate solution, such as that by Bergholz (1978), is to fix attention on a given base flow prescribed by the value of γ and to compute neutral curves in the (A, α)-plane. Critical values of A are then matched to the aspect ratio h through relations of the form (1.1), (1.2). Here it is argued that the stability properties of the convective regime are more usefully described by an analysis based on the assumption that $A \gg 1$ since this is consistent with the basic premise that the ratio A/h is finite. This interpretation leads to the identification of a *universal* neutral curve in the (γ, α)-plane and predicts that instability first occurs for the convective flow corresponding to $\gamma = \gamma_c = 6.30$. Use of the approximate relation (1.2) then implies instability of the slot flow when

$$(A/h)^{\frac{1}{4}} = 2^{\frac{3}{4}}\gamma_c = 10.6, \tag{6.1}$$

a result which seems to be largely in line with experimental observations for a range of aspect ratios (table 1).

Lower and upper branches of the neutral curve stemming from γ_c are found to encompass disturbances ranging from long waves in which $z \sim A$ (which, if relevant, would fill the slot) to shorter finite-aspect-ratio rolls in which $z \sim 1$. The latter type of disturbance concentrates in a critical layer on the centreline as γ increases to the value $\gamma_b = 7.85$ at which the vertical velocity of the base flow reverses. Further analysis is needed to elucidate the properties of the full critical-layer system (5.25) at this point and to extend the upper branch of the neutral curve into the region $\gamma > \gamma_b$ where it is expected that each additional zero of the vertical base flow is accompanied by its own critical-layer structure. Another requirement is the determination of the critical wavelength at γ_c, which is presumably proportional to some positive power of A. The results (3.9) and (5.2) suggest that it is of order $A^{\frac{1}{3}}$ but a complete analysis of the unification of the two branches of the neutral curve near γ_c is required to confirm this and also to incorporate weakly nonlinear effects in a consistent manner. The main findings of the present study are summarized schematically in figure 8.

REFERENCES

Batchelor, G. K. 1954 *Q. Appl. Maths* **12**, 209.

Bergholz, R. F. 1978 *J. Fluid Mech.* **84**, 743.

Daniels, P. G. 1985*a* *Intl J. Heat Mass Transfer* **28**, 2071.

Daniels, P. G. 1985*b* *Proc. R. Soc. Lond.* A **401**, 145.

Daniels, P. G. 1987 *J. Fluid Mech.* **176**, 419.

Elder, J. W. 1965 *J. Fluid Mech.* **23**, 77.

Gill, A. E. & Davey, A. 1969 *J. Fluid Mech.* **35**, 775.

Korpela, S. A., Gozum, D. & Baxi, C. B. 1973 *Intl J. Heat Mass Transfer* **16**, 1683.

Lilly, D. K. 1966 *J. Atmos. Sci.* **23**, 481.

Seki, N., Fukusako, S. & Inaba, H. J. 1978 *J. Fluid Mech.* **84**, 695.

Simpkins, P. G. & Dudderar, T. D. 1981 *J. Fluid Mech.* **110**, 433.

Vest, C. M. & Arpaci, V. S. 1969 *J. Fluid Mech.* **36**, 1.

Wollkind, R. & DiPrima, R. C. 1973 *Phys. Fluids* **16**, 2045.